Resonance Raman Active Vibrations of Rubredoxin. Normal Coordinate Analysis of a 423-Atom Model

Hiroshi SAITO, Takeo IMAI, Kaori WAKITA, Akio URUSHIYAMA,* and Tatsuhiko YAGI†
Department of Chemistry, College of Science, Rikkyo University, Nishiikebukuro 3, Toshima-ku, Tokyo 171
†Department of Chemistry, Shizuoka University, 836 Oya, Shizuoka 422
(Received September 17, 1990)

Normal coordinate analyses were performed on three molecular models of the rubredoxin of *Desulfovibrio vulgaris, Desulfovibrio gigas,* and *Clostridium pasteurianum.* The total 1081, 1093, and 1148 internal coordinates were specified by the X-ray analyzed coordinates of the 390, 399, and 423 atoms, respectively, in a mass-group approximation. The appropriately assumed values of Urey–Bradley force constants as well as some diagonal values of out-of-plane bending and torsional forces gave 146, 146, and 148 normal modes, respectively, in 250—450 cm^{-1} region. These are the deformational vibrations within the peptide skeleton of the protein molecules. The Fe–S stretching displacements of the FeS_4 core contribute to a limited number of these vibrations. The modes having a totally symmetric Fe–S stretching contribution confined within a frequency region of 290—330 cm^{-1} in which the principal resonance Raman band of rubredoxin has been reported, and the several minor resonance Raman bands reported in the higher frequency region of 330—420 cm^{-1} were assigned to noraml modes having a non-totally symmetric Fe–S stretching character. The PED values indicated that all of these modes are constructed mostly by the deformational displacements in the peptide skeleton widely spread into the molecule around the FeS_4 core. This feature is very similar to the case of the blue-copper protein studied previously.

In a previous study,[1] a normal coordinate analysis of the blue-copper protein was carried out on molecular models constructed using a maximum of 169 atoms including the blue-copper site. The analysis showed that the resonance Raman (RR) active modes comprise a dominant contribution of the bond angle bending displacements in the particular part of the peptide skeleton including side chains around the blue-copper site. A sensitive variation in the RR spectra of the type-1 blue-copper proteins was ascribed to a conformational difference in the protein skeleton around the blue-copper site.

In the present study, this work was extended to rubredoxin, which is the initial member of a class of non-heme iron-containing proteins having the simplest Fe–S(cysteine)$_4$ core in the molecule. Long et al.[2,3] first reported the RR effect of oxidized rubredoxin of *Clostridium pasteurianum* in both crystalline and solution phases. The spectra in both phases contain several components: a dominant band (polarized) at 314 cm^{-1}, a moderate band (depolarized) at 368 cm^{-1}, and a weak broad band (depolarized) at 126 cm^{-1} with a shoulder at 150 cm^{-1} upon excitation within a visible Fe←S charge-transfer absorption band centered at 490 nm. Subsequently, Yachandra et al.[4] have found a small shoulder at 325 cm^{-1} in the higher envelope of the main band and an evident splitting by 12 cm^{-1} of the moderate band, commonly found in the RR spectra of rubredoxin of four different bacterial species. They assigned the main band (at 312 cm^{-1}) to the A_1 breathing mode of the FeS_4 core and the shoulder (at 325 cm^{-1}) and the split bands (at 359 and 371 cm^{-1}) to the $B_1+B_2+A_1$ components of the $T_2(T_d)$ Fe–S stretching vibration under the C_{2v} effective symmetry of the core. However, they did not succeed in the reproduction of such a large splitting of the T_2 mode employing any variation of the Urey–Bradley force constant values, considering the actual lowering of the FeS_4 core symmetry in their normal coordinate analyses on a maxinum of thirteen-atom molecular model.

We performed normal coordinate analyses of the molecular models constructed by the three X-ray analyzed molecules of oxidized rubredoxin, from *Desulfovibrio vulgaris* (Rd:Dv),[5] *Desulfovibrio gigas* (Rd:Dg),[6] and *Clostridium pasteurianum* (Rd:Cp),[6] on 390-, 399-, and 423-atom systems, respectively. The results clearly indicated an extensive coupling between the Fe–S stretching vibration and bond angle bending displacements in the polypeptide skeleton widely spread into the molecule around the FeS_4 core. The vibrational characteristics of the RR active modes will be discussed from a different point of view from that by Yachandra et al.[4]

Material and Measurements

Rubredoxin from *Desulfovibrio vulgaris* Miyazaki (Rd:DvM) was isolated as described elsewhere.[18] The 495/280 nm absorbance ratio of the purified protein was ca. 0.4. The RR signals were detected with a backscattering technique from the surface of a dried protein film on a small iron plate which was wholly immensed into liquid nitrogen within a quartz Dewar. All sampling procedures were carried out in an oxygen-free dry box. The Ar^+ 4880 Å line (350 mW) was used as an excitation source. The spectra were well reproduced during a prolonged acquisition time of about eight hours.

Computation

Our view concerning a normal coordinate analysis of protein molecules in which various subsidiary forces work within the molecules was discussed in a

previous study.[1] While the RR effects of rubredoxin appear to be in a somewhat lower wavenumber region (mainly in 290—430 cm^{-1}) than that of the blue-copper proteins (mainly in 360—450 cm^{-1}) previously studied, a similar basis of the approximation, ignoring the hydrogen-bonding potential, charge potential, van der Waals potential, potential due to solvent molecules, and almost of torsional potentials, was also employed in the present study. No particular remark concerning the anharmonicity of the principal RR active vibration of 312 cm^{-1} was reported while assigning the overtone and combination signals. This has been reconfirmed in the present measurement in the overtone region (Fig. 1). The lowest RR bands of rubredoxin detected in 120—160 cm^{-1} region, which were assigned to the S–Fe–S deformational modes ($\nu_2(E)+\nu_4(T_2)$) of the tetrahedral FeS_4 core, must be greatly influenced by the low-frequency "concerted motion" of the protein skeleton, which is believed to have frequencies of up to ca. 100 cm^{-1}. Therefore, the normal coordinates of these deformational modes must not be correctly deduced, although an apparent coincidence between the calculated and observed values could be obtained when the values of the bending and repulsive forces were adjusted. Thus, the discussion is almost limited to within the Fe–S stretching region of vibration studied in the present work.

Totals of 1081 (Rd:Dv), 1093 (Rd:Dg), and 1148 (Rd:Cp) internal coordinates involving all possible bond-stretching and bond-angle-bending coordinates, as well as some selected coordinates of the out-of-plane bending regarding the C_α–C(CO)–N part in the peptide bonding and the CH_n–, OH–(benzene ring) part in the side chain (and the corresponding part in the tryptophan residue) as well as the torsion around N–C_α bond in the peptide bonding, were specified from the X-ray determined 390, 399, and 423 non-hydrogen atoms, respectively. A mass-group approximation in which the mass of all hydrogen atoms is included into those of the attached atoms was employed similarly to the previous work.

The geometrical parameters of the molecules of rubredoxins from *Desulfovibrio vulgaris* (Rd:Dv), *Desulfovibrio gigas* (Rd:Dg) and *Clostridium pasteurianum* (Rd:Cp) consisting of 52, 52, and 54 amino acid residues, respectively, were obtained from the Protein Data Bank (PDB). The primary structure (amino acid sequences) of Rd:Dv is shown in Fig. 4. The Urey–Bradley force constant values as well as diagonal values of the out-of-plane bending and the torsional forces used in the present work are essentially the same as those used in the previous work. The Fe–S(cysteine) stretching force was set to be K(Fe–S)=1.36 mdyn $Å^{-1}$ after several trial calculations to obtain a better fitting to the observed RR spectra. This value is somewhat larger than that proposed by Yachandra et al. This is due to the extensive coupling of the Fe–S stretching

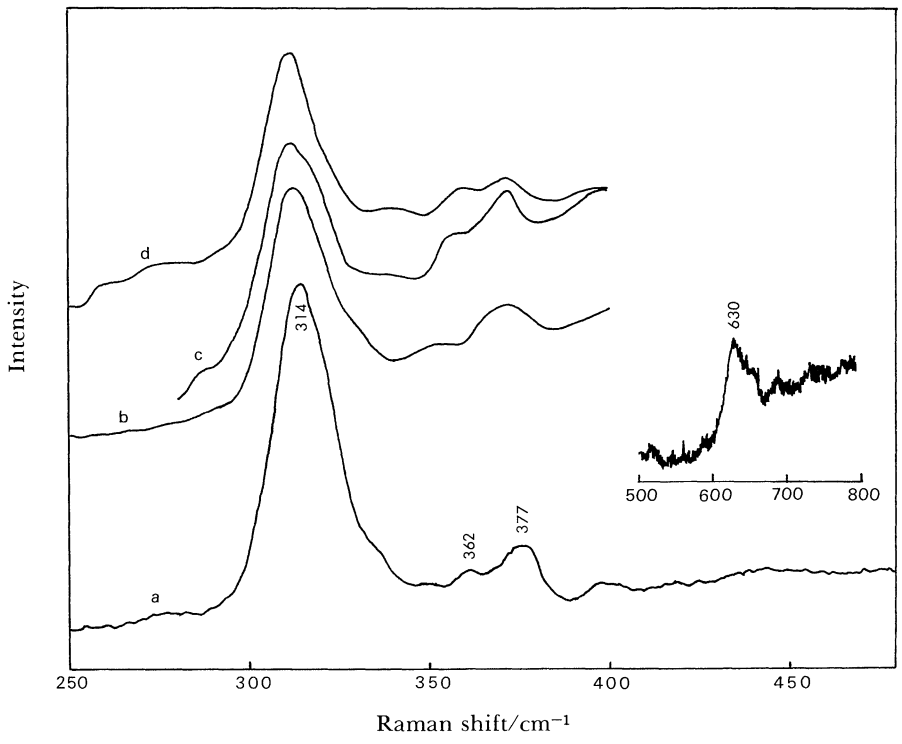

Fig. 1. Resonance Raman spectra of rubredoxin. (a) *Desulfovibrio vulgaris* Miyazaki at 77 K (present measurement). (b) *Megasphera elsdenii*.[4] (c) *Desulfovibrio sulfricans*.[4] (d) *Desulfovibro gigas*.[4]

displacements to the skeletal deformational modes (see below).

The computer programs used for normal coordinate analyses are the same as those used in the previous study. All computational work was done on M682H and S-820 computers at the Computer Center of the University of Tokyo.

Results and Discussion

The resonance and preresonance Raman mechanisms have been discussed in the literature.[7,8] Resonance enhancement is primarily sensitive to a displacement of potential surface of the electronic excited states, which is concerned with the Raman excitation, in totally symmetric normal coordinate space (Albrecht's A term).

The RR spectrum of the oxidized Rd:Dv is shown in Fig. 1, in which the spectra of those from several other bacterial species already reported are also included. The essentially similar spectrum of Rd:Cp has been shown in the literature.[3] The sequence resemblances between the rubredoxins were shown,[10,11] in which, especially, the sequential difference ratio between Rd:Dv and Rd:DvM was found to be only 5/52. The invariant nature in the over-all folding and $Fe-S_4$ environment in the three-dimensional X-ray structures of Rd:Dv, Rd:Cp, and Rd:Dg has also been described.[11] The present measurement confirms the presence of additional weak bands at ca. 397, ca. 420, and ca. 440 cm^{-1}, while the main part of the spectra (290—390 cm^{-1}) is quite similar to those reported for other species. A distinct overtone signal of the main band (314 cm^{-1}) was detected at 630 cm^{-1}.

The excitation profile of the Raman bands of rubredoxin was discussed by Long et al. The characteristic intense absorption bands of oxidized rubredoxin centered at 20000 and 27000 cm^{-1} can be correlated with charge-transfer transitions from the bonding molecular orbitals localized mainly at the sulfur ligands to the non-bonding orbitals of the iron 3d orbitals[9] of the tetrahedral FeS_4 core; the Fe-S displacement must be therefore occur in the totally symmetric normal coordinate space associated with these electronic transitions (elongation of the Fe-S bondings in the

Table 1. Important Normal Mode Frequencies (in 250—450 cm^{-1}) and Their PED Values of Four Fe-S Stretching Coordinates in Rubredoxin[a]

Normal coord.	Frequency	PED[b] of Fe-S stretching coordinates			
	cm^{-1}	Cys6-Fe	Cys9-Fe	Cys39-Fe	Cys42-Fe
Q 616	419.1	−4.33	1.31	6.27	−1.27
Q 617	416.8	19.27	−6.78	−11.06	4.67
Q 621	412.9	18.55	−7.14	−16.66	6.42
Q 622	412.7	−9.84	7.03	3.38	−1.99
Q 623	388.2	12.12	−7.79	32.25	−0.65
Q 637	378.5	1.96	2.99	0.18	−8.29
Q 639	372.7	−1.67	−0.46	4.18	5.61
Q 641	370.5	−0.00	−6.41	1.39	2.91
Q 642	368.4	−3.71	25.71	−4.23	−0.68
Q 647	357.4	−0.47	29.97	−40.48	7.58
Q 649	356.0	−4.18	−1.51	4.10	1.79
Q 651	354.8	−17.98	−0.27	5.57	15.43
Q 652	351.7	6.28	−0.58	0.00	−4.00
Q 655	342.0	1.49	3.17	−0.00	1.61
Q 662	340.2	−0.02	−6.64	0.05	−9.75
Q 664	335.4	−6.16	0.00	4.34	10.21
Q 670	330.9	−4.28	−1.07	−0.41	0.06
Q 672	329.8	13.55	2.74	2.70	−1.46
Q 673	326.1	−11.13	−10.51	−7.35	−3.54
Q 675	322.5	2.69	0.92	1.07	3.27
Q 678	308.3	−0.22	0.88	−1.12	−10.67
Q 690	302.0	5.05	14.55	5.43	10.75
Q 694	293.8	1.27	0.82	1.44	5.41

a) Rubredoxin of *Desulfovibrio vulgaris*: (minus) signs represent the (minus) sign of the corresponding L-matrix elements, l_{in}; only normal vibrations having total PED value of the four Fe-S stretching coordinates exceed 5.8 are presented; Urey-Bradley force constant values are $K(Fe-S)=1.360$ mdyn $Å^{-1}$, $H(Fe-S-CH_2)=0.150$, $F(Fe-S-CH_2)=0.040$, $H(S-Fe-S)=0.085$, $F(S-Fe-S)=0.085$ mdyn $Å^{-1}$, and other skeletal forces were set as the same values as the previous analysis of the blue-copper proteins[1] (see text). b) Definition $PED=(F_{ii}l_{in}^2/\sum F_{ii}l_{in}^2)\times 100$ is employed here.

#) While a correction of Thr21 to Asp21 was pointed out on the basis of the DNA sequence (Ref. 10), the original Thr21 is used here as the X-ray structure of Rd:Dv.

electronic excited state). Therefore, the principal RR effect observed at 314 cm^{-1} upon the visible excitation must be primarily related to the totally symmetric Fe–S stretching component in normal coordinates.

The present calculational evidence can be divided into the following four categories:

(1) The totals of 146 (Q_{594}—Q_{739}) modes for Rd:Dv, 146 (Q_{605}—Q_{750}) for Rd:Dg, and 148 (Q_{634}—Q_{781}) for Rd:Cp were obtained in the RR interesting region of the 250—450 cm^{-1}, respectively. The frequency positions of these normal modes are shown in Figs. 2—4. These modes all comprise, principally, deformational displacements within the peptide skeleton, having a minor contribution of skeletal bond stretching coor-

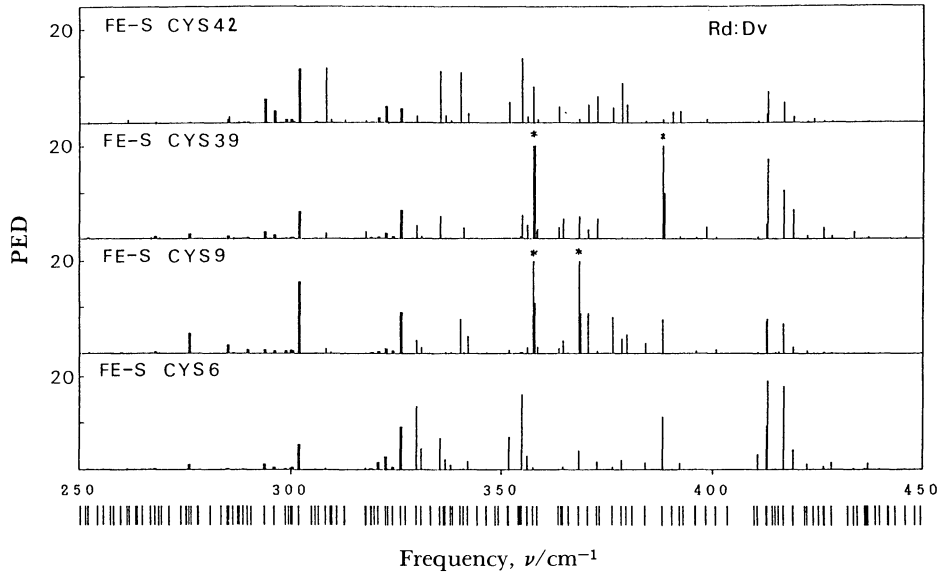

Fig. 2. PED of the four Fe–S stretching coordinates of Rd : Dv. The bold and thin lines denote the normal modes including totally symmetric (with all the same sign of the corresponding L-matrix elements, L_{in}) and non-totally symmetric (with not the same sign) of Fe–S stretching displacements, respectively. The short vertical lines below each figures denote the frequency positions of the normal vibrations. The values exceed 20.0 (asterisked) are depicted by double lines.

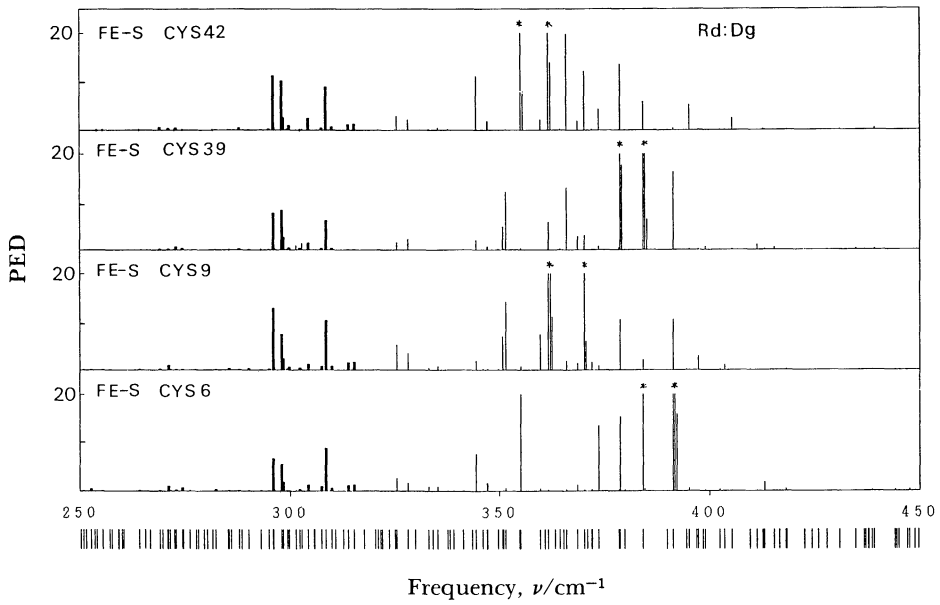

Fig. 3. PED of the four Fe–S stretching coordinates of Rd : Dg. The notation is similar to Fig. 1.

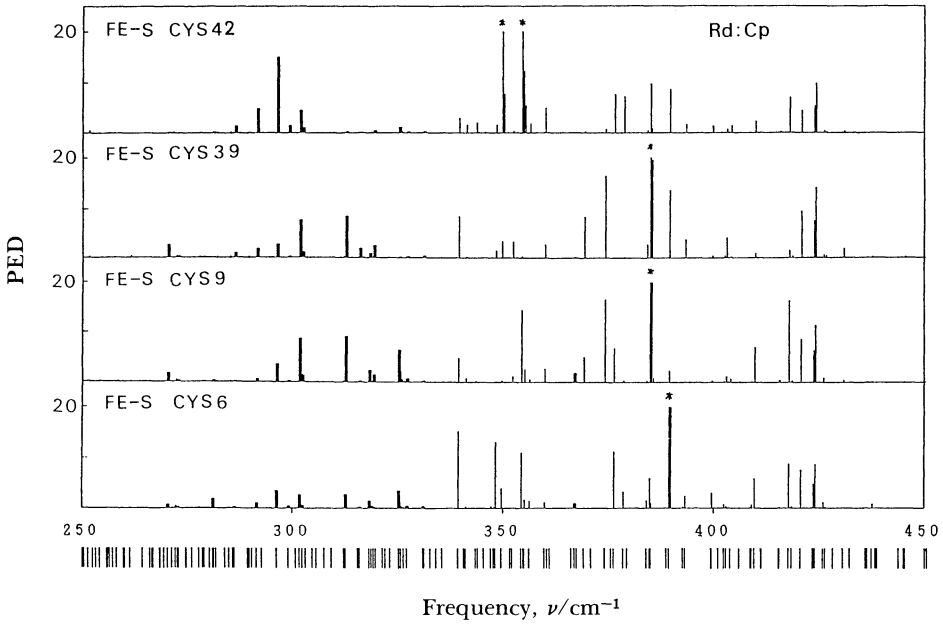

Fig. 4. PED of the four Fe–S stretching coordinates of Rd : Cp. The notation is similar to Fig. 1.

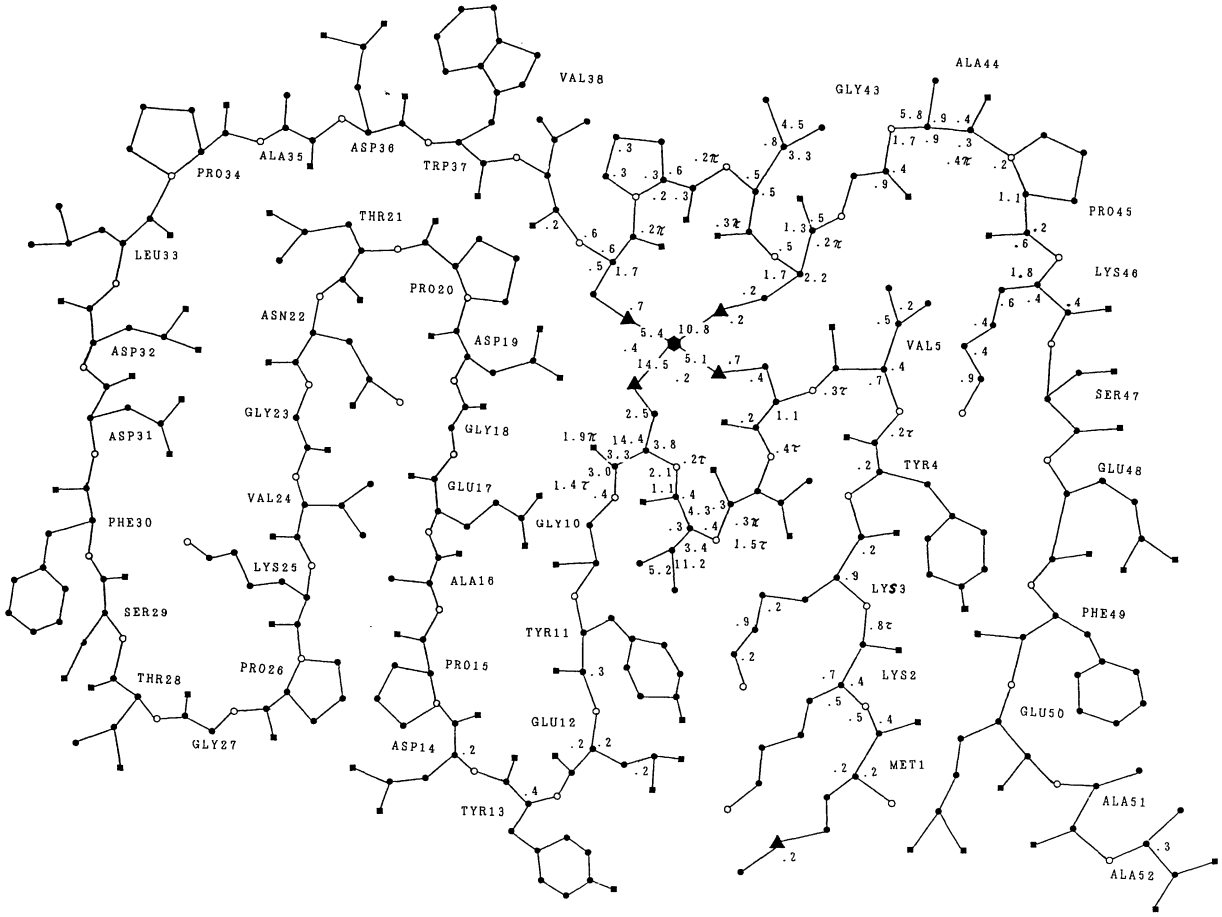

Fig. 5. PED values of the deformational coordinates (bond angle bending, out-of-plane bending: π, and torsional: τ) of the Q_{690} (302.0 cm^{-1}) of Rd : Dv (●: carbon; □: oxygen; ○: nitrogen; ▲: sulfur; ⬢: iron). The values exceed 0.2 are depicted.

dinates (vide infra).

(2) Among the above-mentioned normal vibrations, limited modes involve an actual contribution of the Fe–S stretching displacements (Table 1). In Figs. 2—4. are illustrated the PED values of the four Fe–S(cysteine) stretching coordinates for the normal modes in the 250—450 cm^{-1} region. There is no mode which comprises almost a pure contribution of the Fe–S stretching vibration.

(3) The normal modes involving a totally symmetric Fe–S stretching character, which means in the present study those modes having the same sign as all four corresponding L-matrix elements, appear in the lower-wavenumber region (280—330 cm^{-1}) than those of the non-totally symmetric Fe–S stretching character (not the same sign of all the four corresponding L-matrix elements) (330—450 cm^{-1}). The frequency positions of the former have been confined in the region where the principal RR band was observed, as shown in Fig. 1. The latter well interprets the minor RR bands appearing in the higher-frequency region (including the newly detected bands in the present measurement). An interpretation of the RR intensity of the non-totally symmetrical Fe–S stretching vibrations is possible if the actual reduction of the FeS_4 core symmetry is taken into account. In fact, the 1.2 Å refined X-ray structure of Rd:Cp indicates the smallest and largest S–Fe–S angles of 103.7(4) and 114.3(4) degree and the shortest and longest Fe–S bond lengths of 2.24(1) and 2.39(1) Å, respectively. In C_1, the actual symmetry of the FeS_4 core, all vibrational modes can be RR enhanced.

(4) Normal vibrations having a large (totally or non-totally symmetric) Fe–S stretching contribution comprise skeletal deformational displacements over a considerably wide range of the protein skeleton around the FeS_4 center. The PED values of the 302.0 cm^{-1} mode of Rd:Dv, for example, which has the largest totally-symmetric Fe–S stretching character, are depicted in Fig. 5; the PED values of the bond-angle-bending coordinates (including out-of-plane bending and torsion) summed up for the four normal modes having a large Fe–S stretching character are shown in Fig. 6. Essentially similar figures were obtained for the non-totally symmetric Fe–S stretching vibrations (Fig. 7). It was found that the interaction occurs with the deformational coordinates, roughly speaking, in more than 15 amino acid residues around the FeS_4

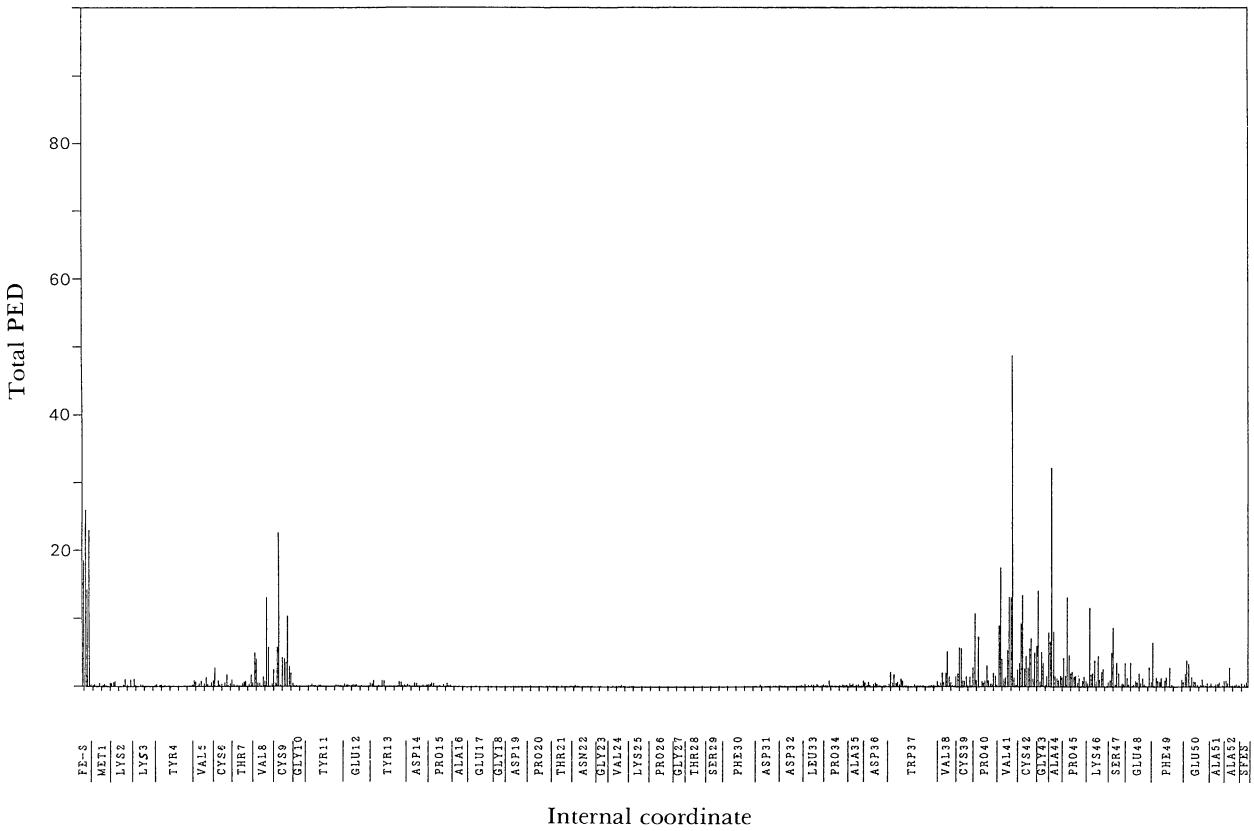

Fig. 6. PED of the deformational coordinates defined in the amino acid residues in the primary structure of Rd : Dv. The Fe–S stretching and S–Fe–S bending coordinates are included at the first top and the last end of the internal coordinates, respectively. The values depicted are those summed up the four normal modes, Q_{673} (326.1 cm^{-1}), Q_{675} (322.5), Q_{690} (302.0), and Q_{694} (293.8) which involve totally symmetric displacements of the Fe–S stretching coordinates.

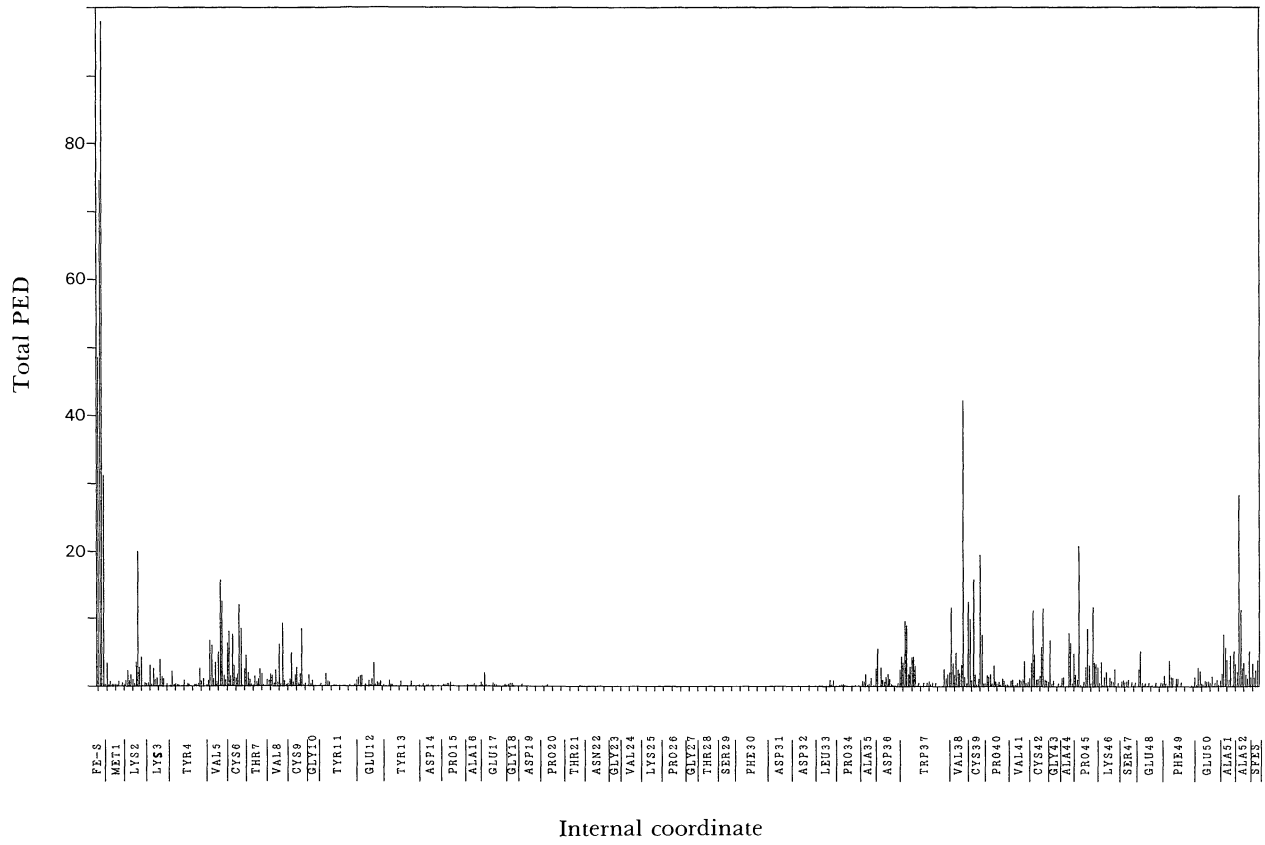

Fig. 7. PED of the deformational coordinates Rd : Dv. The notation is similar to Fig. 4. The values depicted are those summed up the six normal modes, Q_{621} (412.9 cm^{-1}), Q_{623} (388.2), Q_{642} (368.4) and Q_{647} (357.4), Q_{652} (351.7), Q_{664} (335.4) which involve non-totally symmetric displacements of the Fe–S stretching coordinates.

center. The PED ratio of the skeletal bond stretching, (four) Fe–S stretching and skeletal bending coordinates (including out-of-plane bending and torsion) is 8.99:35.77:55.24 for the Q_{693} (302.0 cm^{-1}) modes of Rd:Dv. These strong cooperations between Fe–S stretching and skeletal deformational displacements are not accidental with the particular set value of the force constants. We carried out many trial calculations in which all of the force constant values were either increased or decreased from the original force constant set, while the K(Fe–S) and H, F(S–Fe–S) values are kept constant. Extensive mixing between the Fe–S stretching and the bond angle bending displacements always appeared. In other words, the vibrational characteristics mentioned above, (1)—(4), are retained unless extraordinary small values of the skeletal deformational force constants are employed.

Conclusion

The present assignments differ from those reported by Yachandra et al. regarding the following two points:

(1) The main band at 312 cm^{-1} including the shoulder at ca. 325 cm^{-1}, is assigned to skeletal deformational vibrations having totally symmetrical Fe–S stretching displacements confined to within this frequency region. Moderate bands at ca. 360 and ca. 370 cm^{-1} and newly detected bands in the 390—450 cm^{-1} region are the skeletal deformational modes having non-totally symmetrical Fe–S stretching contributions. Whereas, Yachandra et al.[18] assigned the main band at 312 cm^{-1} to the FeS_4 breathing modes and the shoulder at ca. 325 cm^{-1} and the moderate peaks at ca. 360 and ca. 370 cm^{-1} to split components (B_1+B_2+A_1) of the degenerate (T_2:T_d) Fe–S stretching vibration in the C_{2v} effective symmetry of the FeS_4 core. Still, they were puzzled by such a large splitting of the $T_2(T_d)$ vibration.

(2) They suggested the importance of coupling between Fe–S stretching and the Fe–S–C_β (cysteine) and/or S–C_β–C_α (cysteine) bending displacements in order to account for the extraordinary large splitting of the B_1+B_2+A_1 components, in addition to accounting for the actual reduction of the FeS_4 core symmetry. The nearly planer geometry of the Fe–S–C_β–C_α sequences present in the proteins has been considered to be advantageous for these couplings. However, our calculational results show no particular impor-

tance of these couplings (Figs. 3—5). They do evidence an extensive coupling between the Fe–S stretching and skeletal deformations around the FeS_4 core.

Though a precise determination of the normal coordinates of the large molecules of the proteins is not the present purpose, a new standpoint for understanding the RR spectra of the rubredoxins is presented regarding the extensive mixing of the Fe–S stretching and the skeletal deformational displacements in the peptide skeleton around the FeS_4 core. The resonance Raman spectroscopy has been believed to constitute the most poweful method for identifying the iron–sulfur core in ferredoxins.[12–17] However, there are still problems remaining to be analyzed: for example, concerning the not negligible difference in the RR spectra between the ferredoxin from spinach and adrenodoxin,[13] both of which were proven to have similar Fe_2S_6 cluster, and in the RR spectra of the 4Fe-type ferredoxins and HiPIP-type,[16] especially, in the higher wavenumber Fe–S(terminal thiolate) stretching region of 350—400 cm^{-1}. This work will be extended to ferredoxins which contain a multi-iron cluster. A theoretical base for a further utilization of the RR spectroscopy will also be developed.

References

1) A. Urushiyama and J. Tobari, *Bull. Chem. Soc. Jpn.*, **63**, 1563 (1990).

2) T. V. Long, II and T. M. Loehr, *J. Am. Chem. Soc.*, **92**, 6384 (1970).

3) T. V. Long, II, T. M. Loehr, J. R. Allkins, and W. Lovenberg, *J. Am. Chem. Soc.*, **93**, 1809 (1971).

4) V. K. Yachandra, J. Hare, I. Moura, and T. G. Spiro, *J. Am. Chem. Soc.*, **105**, 6455 (1983).

5) E. T. Adman, L. C. Sieker, L. H. Jensen, M. Bruschi, and J. LeGall, *J. Mol. Biol.*, **112**, 113 (1977).

6) K. D. Watenpaugh, L. C. Sieker, and L. H. Jensen, *J. Mol. Biol.*, **138**, 615 (1980).

7) M. Tsuboi and A. Hirakawa, *J. Raman Spectrosc.*, **5**, 75 (1976).

8) T. G. Spiro and P. Stein, *Ann. Rev. Phys. Chem.*, **28**, 501 (1977).

9) J. V. Pivnichny and H. H. Brintzinger, *Inorg. Chem.*, **12**, 839 (1973).

10) F. Shimizu, M. Ogata, T. Yagi, S. Wakabayashi, and H. Matsubara, *Biochimie*, **71**, 1171 (1989).

11) M. Frey, L. Sieker, F. Payan, R. Haser, M. Bruschi, G. Pepe, and J. Legall, *J. Mol. Biol.*, **197**, 525 (1987).

12) R. W. Lane, J. A. Ibers, R. B. Frankel, G. C. Papaefthymiou, and R. H. Holm, *J. Am. Chem. Soc.*, **99**, 84 (1977).

13) V. K. Yachandra, J. Hare, A. Gewirth, R. S. Czernuszewicz, T. Kimura, R. H. Holm, and T. G. Spiro, *J. Am. Chem. Soc.*, **105**, 6462 (1983).

14) R. W. Lane, J. A. Ibers, R. B. Frankel, and R. H. Holm, *Proc. Nat. Acad. Sci. USA*, **72**, 2868 (1975).

15) J. -M. Moulis, J. Meyer, and M. Lutz, *Biochemistry*, **23**, 6605 (1984).

16) R. S. Czernuszewicz, K. A. Macor, M. K. Johnson, A. Gewirth, and T. G. Spiro, *J. Am. Chem. Soc.*, **109**, 7178 (1987).

17) M. K. Johnson, R. S. Czernuszewicz, T. G. Spiro, J. A. Fee, and W. V. Sweeney, *J. Am. Chem. Soc.*, **105**, 6671 (1983).

18) S. Han, R. S. Czernuszewicz, and T. G. Spiro, *J. Am. Chem. Soc.*, **111**, 3496 (1989).

19) M. Frey, L. Sieker, F. Payan, R. Haser, M. Bruschi, G. Pepe, and J. L. Gall, *J. Mol. Biol.*, **197**, 525 (1987).